JACS
JOURNAL OF THE AMERICAN CHEMICAL SOCIETY
Article
pubs.acs.org/JACS

The Structural Basis for Enhanced Silver Reflectance in Koi Fish Scale and Skin

Dvir Gur,[†] Ben Leshem,[‡] Dan Oron,[‡] Steve Weiner,[†] and Lia Addadi*[,†]

Departments of [†] Structural Biology and [‡]Physics of Complex Systems, Weizmann Institute of Science, Rehovot, 76100, Israel

Supporting Information

ABSTRACT: Fish have evolved biogenic multilayer reflectors composed of stacks of intracellular anhydrous guanine crystals separated by cytoplasm, to produce the silvery luster of their skin and scales. Here we compare two different variants of the Japanese Koi fish; one of them with enhanced reflectivity. Our aim is to determine how biology modulates reflectivity, and from this to obtain a mechanistic understanding of the structure and properties governing the intensity of silver reflectance. We measured the reflectance of individual scales with a custom-made microscope, and then for each individual scale we characterized the structure of the guanine crystal/cytoplasm layers using high-resolution cryo-SEM. The measured reflectance and the structural-geometrical parameters were used to calculate the reflectance of each scale, and the results were compared to the experimental measurements. We show that enhanced reflectivity is obtained with the same basic guanine crystal/cytoplasm stacks, but the structural arrangement between the stack, inside the stacks, and relative to the scale surface is varied when reflectivity is enhanced. Finally, we propose a model that incorporates the basic building block parameters, the crystal orientation inside the tissue, and the resulting reflectance and explains the mechanistic basis for reflectance enhancement.

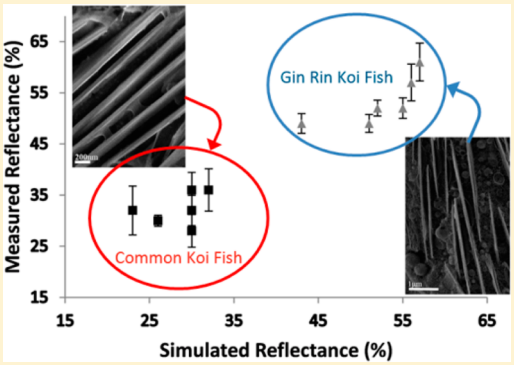

INTRODUCTION

The physical basis of multilayer reflectors for producing structural colors in biological systems in general and in fish scales in particular is well established.[1−5] However, one interesting open question is how fish modulate the reflectivity of their silver scales. Answering this question can not only improve our mechanistic understanding of reflectance intensity in biological multilayer reflectors but may also provide new insights into ways in which reflectance can be enhanced in synthetic systems.

In nature structural colors are extensively used by different organisms for a variety of functions, such as visual communication for species recognition, mimicry and camouflage, and in the eyes for vision enhancement.[6−13] The physical phenomenon responsible for structural colors is constructive interference of selected wavelengths of reflected light, originating from the interaction of light with periodic structures that have physical dimensions similar to the wavelength of light. The phenomenon of structural colors was first described by Hooke in 1665 in his book *Micrographia*,[14] but a better understanding of these structures was achieved with the development of the electron microscope in the 20th century. The physical interpretation of the phenomenon, however, has not changed since the multilayer interference approach was calculated by Lord Rayleigh in 1887.[15−17]

A multilayer reflector array consists of alternating layers of transparent materials with different refractive indices. The array can act as a reflector when the optical thickness nd (the product of the physical thickness d and the refractive index n) of all layers is comparable to the wavelength of light. The light reflected from the different layers undergoes constructive interference for some wavelengths and destructive interference for others, resulting in distinct colors being observed. As the angle of incident light changes, different wavelengths constructively interfere, and the colors change.[18,19] Probably the most common example of multilayer reflectors is the metallic-like glitter observed from the scales of many types of fish. This silvery reflectance is generated by broadband, wavelength-independent reflectance over the entire spectrum of visible light.[2] In fish this reflectance is produced by alternating layers of high refractive index thin plate-shaped guanine crystals (with n = 1.83 along the axis normal to the biogenic plate axis) and low refractive index cytoplasm (dominated by that of water, n = 1.33).[4,20] The guanine crystals in fish are intracellular: they form inside specialized cells called iridophores,[21,22] located underneath the scales and in the stratum argentum, a subdermal layer of the skin.[3,5,23] In both locations each crystal forms inside a crystal chamber composed of a lipid bilayer.[22] Recent studies have shown that the formation of these crystals occurs via an amorphous precursor phase of guanine.[24]

One well-studied example of silver reflectance in fish is the Japanese Koi fish (*Cyprinus carpio*) that has scales with a metallic luster as well as pigmented colors.[24−26] One variety, the Gin Rin Platinum Ogon Koi (Figure 1b, termed Gin Rin in this work) has

Received: September 16, 2014
Published: November 13, 2014

Figure 1. Koi fish belong to the Cyprinidae, *Cyprinus carpio*. (a) Platinum Ogon, termed "Common" in this study. (b) Gin Rin Platinum Ogon, termed Gin Rin in this study. The Gin Rin variety has extra reflectance seen mostly from the scales on the two sides of the dorsal fin. Length of fish is approximately 25 cms.

scales usually located on both sides of the dorsal fin, with strikingly higher reflectance than the more common Platinum Ogon Koi (Figure 1a, termed "Common" in this work). In the experiments presented here, we compare the highly reflecting Gin Rin scales with the Common scales. Due to the variability in reflectance between different scales we had to develop a correlative method which allowed us to measure the reflectance of individual scales and to characterize the structural parameters of the crystal/cytoplasm layers of the same scales. For the latter we used cryo-SEM in order to avoid dehydration artifacts that would change the thickness of the highly hydrated cytoplasm layers. Using this approach we were able to identify the parameters responsible for the variations in reflectance. The agreement between the reflectance intensity and spectral distribution simulated from these parameters, and the measured reflectance spectrum, confirms the validity of the derived model.

RESULTS

The reflectance of scales of around 3 × 4 mm^2 was measured from 2 Common Koi and 2 Gin Rin Koi (3 scales from each fish) within 1 h after extraction of the scale from the fish. We used a custom built microscope to measure the reflectance that enabled us to acquire the reflectance spectrum and the image of the scale with the associated epidermal layer, at the same location. The image showed the distribution of the reflected light over the scale surface. Immediately after making the reflectance measurements, the reflective areas of the same scale were high-pressure frozen and subsequently observed using the cryo-SEM. All of the results are shown in Table 1.

Table 1. Summary of All of the Parameters Measured by Cryo-SEM and by the Custom Built Microscope[a]

fish no.	(a) crystal thickness (nm)	(b) cytoplasm thickness (nm)	(c) orientation of the crystals relative to the scale (°)	(d) no. of iridophores in a cross section	(e) coverage area (%)	(f) measured reflectance (%)	(g) measured normalized reflectance (%)	(h) simulated reflectance (%)
GR 1.1	28 ± 8 (n = 98)	96 ± 61 (n = 63)	5 ± 5.5 (n = 51)	4−5	88	46	52	52
GR 1.2	26 ± 7 (n = 39)	108 ± 42 (n = 54)	2 ± 2 (n = 30)	4−5	86	42	49	51
GR 1.3	28 ± 5 (n = 39)	86 ± 43 (n = 44)	2 ± 2.5 (n = 43)	3−4	80	37	49	43
GR 3.1	34 ± 10 (n = 49)	101 ± 56 (n = 130)	3.5 ± 2.5 (n = 98)	4	82	42	52	55
GR 3.2	29 ± 8 (n = 32)	108 ± 50 (n = 52)	3 ± 3 (n = 42)	4−5	91	52	57	56
GR3.2	20 ± 6.6 (n = 33)	107 ± 70 (n = 38)	2 ± 2 (n = 32)	4−5	89	54	61	57
Co 2.1	30 ± 8 (n = 51)	165 ± 51 (n = 100)	30.5 ± 6.5 (n = 85)	1−2	60	23	36	32
Co 2.2	26 ± 5 (n = 48)	175 ± 68 (n = 39)	26.5 ± 5 (n = 62)	1−2	53	19	36	30
Co 2.3	27 ± 5 (n = 42)	165 ± 51 (n = 100)	25.5 ± 3.5 (n = 45)	1−2	51	14	28	30
Co 4.1	31 ± 10 (n = 51)	170 ± 82 (n = 45)	35 ± 8 (n = 56)	1−2	62	19	30	26
Co 4.2	28.5 ± 7 (n = 32)	164 ± 74 (n = 69)	30.5 ± 7.9 (n = 51)	1	60	19	32	23
Co 4.3	28.5 ± 8 (n = 35)	155 ± 82 (n = 43)	24.5 ± 6 (n = 42)	1−2	66	21	32	30

[a]Summary of all of the parameters measured by cryo-SEM (a−d) and by the custom built microscope (e−g) that were used for simulations and normalization of the reflectance of 12 different scales and skins from both Gin Rin (GR) and Common (Co) Koi. Numbers, e.g., GR 1_1, designate the fish and the scale referred to, respectively. The values measured from the cryo-SEM (a−d) are means for n specimens of high-pressure frozen, freeze fractured scales and skins. (e) Crystal stack coverage area determined from the light microscope images. (f) Integrated measured reflectance determined with a microspectrophotometer and normalized to an Ag mirror. (g) Integrated normalized reflectance, obtained by normalizing the measured reflectance according to the crystal stack coverage area. (h) Simulated reflectance calculated using the parameters measured with cryo-SEM.

dx.doi.org/10.1021/ja509340c | J. Am. Chem. Soc. 2014, 136, 17236−17242

Cryo-SEM. We found that in both the Common and the Gin Rin scales the guanine crystals are uniformly thick plates, with crystal thicknesses ranging from 26 to 31 (±26%) nm for Common and 21 to 34 (±26%) nm for Gin Rin, i.e., with no significant difference between the two groups (Table 1a). However, the average cytoplasm thicknesses of the Gin Rin Koi range from 86 to 108 nm (±50%), and the average cytoplasm thicknesses of the Common Koi range from 155 to 175 nm (±41%), and hence there is a significant difference between the two groups. Note too that the ranges of cytoplasm thicknesses are very large in both Common and Gin Rin Koi, but are much larger in the Gin Rin Koi compared to the Common Koi. As there is not perfect control on the orientation of the fracture plane that is observed in the cryo-SEM images, both measured crystal and cytoplasm thicknesses may be slightly biased by an oblique fracture. We note, however, that the same uncertainty affects the Common and the Gin Rin Koi measurements in a similar manner. Furthermore, the effect is rather small and falls within the standard deviation of the thicknesses.

For both systems, we found a nearest-neighbor mathematical correlation between the spacings of adjacent crystals of 60%, i.e., the spacings of adjacent crystals within a stack are much closer in value than those in different stacks (Figure 1S). There are approximately 25 crystals/cell in the Common Koi, whereas the number of crystals/cell in the Gin Rin Koi is approximately 40 (Figure 2).

We have identified several additional major features in the organization of the crystals in the Gin Rin scales and skins that are different from those of the Common scales and skins. The first difference is in the orientation of the crystals relative to the scale surface and hence relative to the light source. While the majority of the guanine crystals in the Common Koi scale and skin are oriented around a mean value of 30° to the scale surface (Table 1c, Figures 2a and 3a), the crystals in the Gin Rin are usually parallel to the scale surface (Table 1c, Figures 2b and 3c).

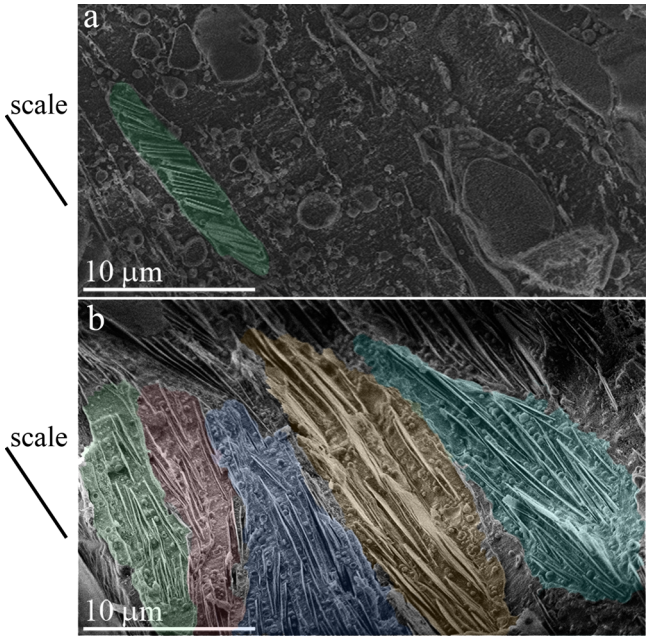

Figure 2. Cryo-SEM micrographs of high-pressure frozen and freeze fractured scales and skin, showing the orientations of the crystals relative to the scale and the number of iridophores in a cross section. Different cells are delimited with different colors. (a) Iridophore cells from a Common Koi; there is only one layer of iridophores, and in this layer the majority of the crystals form an angle around a mean value of 30° to the scale surface. (b) Iridophore cells from a Gin Rin scale; the majority of the crystals are almost parallel to the scale, and there are up to five layers of iridophores in the cross section. Black lines indicate the direction of the scale surface.

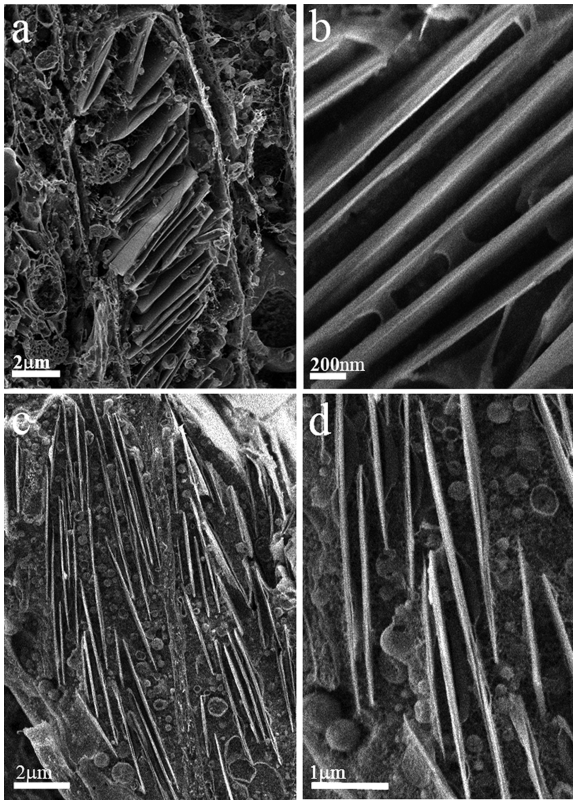

Figure 3. Cryo-SEM micrographs of high-pressure frozen, freeze fractured scale and skin. (a,b) Iridiphore of a Common Koi fish, with one stack of parallel crystals. (c,d) Iridophore of a Gin Rin Koi fish showing two crystal stacks inside a single cell. The crystal stacks often interdigitate resulting in shorter and larger distances between the crystals: the interdigitated stacks have typical intercrystal distance of ∼60 nm, whereas the primary stacks have distances of ∼140 nm.

The second important difference is that the Gin Rin has many more iridophores in the skin and each iridophore usually contains more crystals compared to the Common Koi. In the skin of the Common Koi there is usually only one layer of iridophores underneath the scale, and the iridophore contains one stack of crystals (Table 1d, Figures 2a and 3a). In the Gin Rin skin there are up to 5 iridophores in a cross section, and within each iridophore there are 2−3 crystal stacks (Table 1d, Figures 2b and 3c). This arrangement results in a much larger number of alternating crystal−cytoplasm layers in the scales and skins of the Gin Rin relative to the scales and skins of the Common Koi. Furthermore, inside a Gin Rin iridophore there are multiple crystal stacks leading to interdigitation between the crystals of neighboring stacks (Figures 2b and 3c,d). The interdigitation has several consequences: locally reducing the average thickness of the cytoplasm spacing between the crystals and introducing more disorder into the system both by the variation in cytoplasm spacings and in the angles between adjacent crystals (Figures 2b and 3c,d); factors which have a profound effect on the intensity of reflectance. We confirmed these differences by analyzing an additional eight Gin Rin scales and seven common scales from

dx.doi.org/10.1021/ja509340c | J. Am. Chem. Soc. 2014, 136, 17236−17242

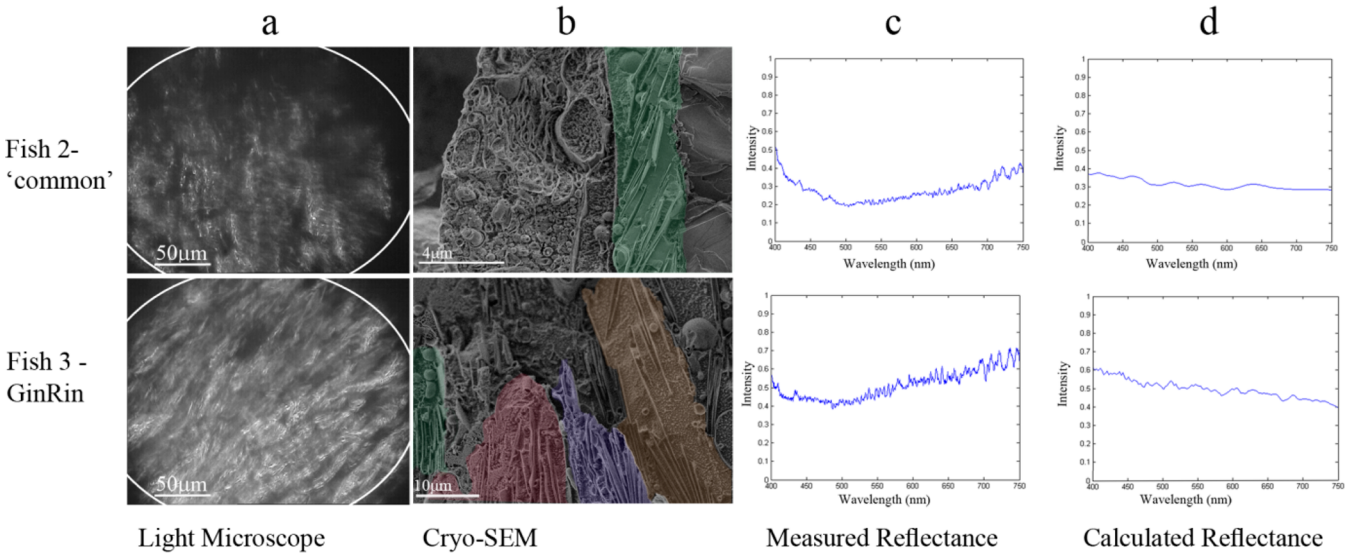

Figure 4. Correlative representation of all the parameters measured or simulated for one Gin Rin scale (fish 3, scale 1) and one Common scale (fish 2, scale 3). (a) Light microscope images. (b) cryo-SEM images, different cells are delimited with different colors. (c) Normalized measured reflectances. (d) Simulated reflectances.

three different fish using the cryo-SEM (Supporting Information).

Measured vs Calculated Reflectance. To calculate the simulated reflectance of each scale (Table 1h and Figure 4), we took into account the mean measured values and standard deviations of the crystal thicknesses, the cytoplasm spacings, the number of iridophores, the number of crystal stacks, and the orientations of the crystals relative to the scale surface. The simulation was based on Monte Carlo transfer matrix calculations (see Experimental Section). Figure 4 shows one example from a Common Koi scale and one from a Gin Rin scale for each of these parameters and the corresponding reflectance measurements, and Table 1 shows the data for each of the 12 different scales measured.

Overall, the reflectance measurements show that both Common and Gin Rin scales exhibit a broad band reflectance typical of a "silvery" iridescence. The measured reflectance of the Gin Rin scales is 2−3 times higher than the reflectance measured for the Common Koi scales (both normalized to the reflectance of a silver mirror, Table 1f). The skin underneath the scale of the Gin Rin appears much more densely covered with crystal stacks (coverage area 80−90%) relative to the skin of the Common Koi (coverage area 50−60%) (Table 1e and Figure 4). However, normalizing the reflectance of the skin and scales to the coverage area of the crystal stacks still results in reflectance values 1.5−2 times higher for the scales and skins of the Gin Rin relative to the Common scales and skins (Table 1g and Figure 4). Therefore, the additional reflectance obtained after normalization to the coverage area is due to the intrinsic structure and photonic properties of the Gin Rin scales and skin. When comparing the simulation calculated for each scale and skin (based on the structural information obtained from the cryo-SEM) to the reflectance measured from the same scale, one can see that the simulated reflectance fits well the broad band reflectance spectrum measured from the scales and skins. One example is shown in Figure 4, and the data for the correlative comparison for all of the measured scales is shown in Table 1. Figure 5 shows a plot of measured vs simulated reflectance for each of the 12 scales, with good agreement between the measured reflectance

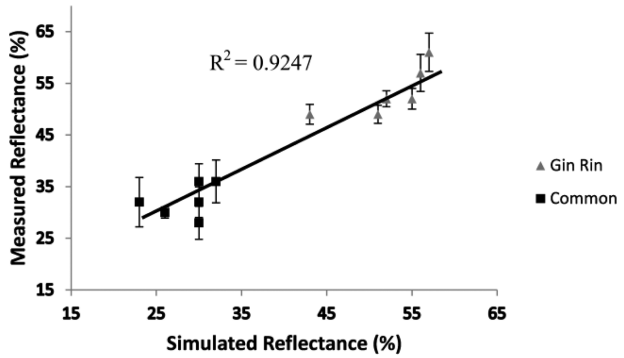

Figure 5. A diagram showing the measured reflectance from 12 scales and skins (6 Gin Rin and 6 Common) vs the simulated reflectance; the reflectance of each scale and skin was measured at three different locations and is represented at each point as standard deviation from the mean. The measured reflectances were obtained by a microspectrophotometer and were normalized according to the crystal stack coverage area in the scales (determined by the light microscope image). The photonic parameters used to simulate the reflectance were determined by cryo-SEM; the parameters that were used are specified in Table 1.

and the simulated reflectance. Clearly both the measured and the simulated values of the reflectance of the Gin Rin scales are much higher than that of the Common scales (50−61% reflectance for the Gin Rin scale and skin and 28−36% reflectance for the Common scale and skin).

DISCUSSION

We show that the additional reflectance in the Gin Rin Koi skin and scales compared to that of the Common Koi skin and scales is caused not only by producing more iridophores but also by structural variations in the architecture of the multilayer reflectors. Thus, the same building blocks are used, but reflectance enhancement is achieved by varying the structure. We identified four different structural features that distinguish the Gin Rin from the Common Koi: (1) The skin underneath the scale of the Gin Rin is much more densely covered with crystal stacks; (2) the orientation of the crystals is almost parallel to the

dx.doi.org/10.1021/ja509340c | J. Am. Chem. Soc. 2014, 136, 17236−17242

scale surface in the Gin Rin, whereas the crystals form an angle of 30° to the scale surface in the Common Koi; (3) the number of layers of iridophores underneath the scale and the number of crystal stacks inside iridophores are much higher in the Gin Rin; (4) interdigitation between the different crystal stacks within the iridophores, and consequently a much wider distribution of *d*-spacings between the crystals, is found in the Gin Rin relative to the Common Koi.

We also show that when taking into account only the differences in the crystal-covered area of the scale, the Gin Rin still has much higher reflectance than the Common Koi scale. This extra reflectance was measured and simulated (Table 1 and Figure 4). The good agreement between the simulated reflectance spectrum and the measured reflectance spectrum confirms that the additional specific features observed in the Gin Rin structure all contribute to the extra reflectance. These are as follows: The effect of more alternating layers in the Gin Rin structure results in higher reflectance. The parallel orientation of the crystals in the Gin Rin system relative to the scale surface causes incident light to enter the crystal stacks at a higher angle than in the case of the inclined crystal stacks in the Common system, reducing the effective thickness of the layers. This arrangement also results in higher reflectance. The interdigitation of the crystal stacks reduces the average spacing between the crystals and results in more crystals per unit area. Furthermore, the interdigitation of the crystal stacks inside the iridophores results in areas in the scale in which the spacing between the crystals is quite small, i.e., 60 nm, together with other areas in which interdigitation does not occur, resulting in a spacing of around 140 nm. These irregularities in the structure contribute to the overall disorder of the system. The above changes in stack ultrastructure, including the introduction of "controlled" disorder, constitute the strategy adopted by the Gin Rin Koi to obtain enhanced reflectivity using the same building blocks, while keeping the thickness of the dermal layer underneath the scale within a similar range.

In both the Gin Rin and the Common systems, the optical thickness of the alternating layers deviates strongly from an ideal reflector. Simulation of the reflectance of an ordered system using the spacings that we have measured results in low (∼10%) reflectivity, when considering 20 alternating layers. Only after introducing the large standard deviation and the irregularities in the structure does the reflectivity increase. Denton and Land proposed that the silver color of certain fish scales and skin could be explained either by a randomly distributed thickness of the different layers or by systematically changing thickness.[27] In a later study on the silvery reflectance of fish, McKenzie et al. described the fish skin as a chaotic system in which the thicknesses of both the high and low refractive index layers are randomly distributed.[2] It was also suggested that neutralization of the polarization of reflection is an important factor in determining the reflective properties of fish skin.[28]

In this study we have found that both ordered and disordered features are present in the structure. The thickness of the cytoplasm spacings is highly variable, whereas the guanine crystals are much thinner and have a much narrower thickness distribution compared to the cytoplasm layers. The same narrow distribution of crystal thicknesses was found for the different scales and skins examined, Gin Rin or Common. Different organisms that use guanine in their reflective systems, such as in the eye of the spider *Drassodes cupreus* and the silvery integument of the spider *Tetragnatha montana*, also show a similar narrow distribution of thicknesses of the guanine crystals and a broader distribution of the cytoplasm spacings.[26,29]

Use of guanine crystals of 60−70 nm thickness, with an optical thickness close to quarter wavelength, would substantially increase the reflectance of the fish scales. However, the crystal thickness in the Gin Rin does not change. The crystal thickness appears to be either genetically determined or reflects the mode of formation. The Gin Rin therefore adopted other structural solutions to achieve higher reflectance. In the spider *Tetragnatha montana*, thicker crystals are produced, but these are composed of ∼20 nm thick crystals separated by a 30 nm layer of amorphous guanine. In this way the crystals have a thickness which is close to the quarter wavelength optical thickness (∼70 nm* 1.83 ≈ 130).

The larger distribution of thicknesses for the cytoplasm is not compatible with systems that produce specific structural colors, such as in the carapace of the copepod Sapphirina male[30,31] or in the dynamic lateral stripe of the Neon Tetra fish.[32−34] In these systems the thicknesses of both the guanine crystals and the cytoplasm spacings are expected to be much more regular, in order to achieve a peak reflectivity at specific wavelengths.

Most of the early pioneering studies describing the reflecting system in fish with silver scales, in which the thicknesses of the guanine crystals were measured, reported that the thicknesses are widely and randomly distributed. It has to be taken into account, however, that the techniques used resulted in the crystals being completely dissolved or lost, such that what was actually measured were the cavities left after crystal dissolution, which were distorted during drying and cutting. The latter may also have disturbed the cytoplasm layer thicknesses. We believe that these are the reasons why these studies resulted in much larger values of thickness for the guanine crystals. We still do not completely understand the mechanism of formation of these intracellular guanine crystals and what exactly determines their size, but the fact that different systems produce crystals with similar shape and sizes suggests that there is a common mechanism of formation.

A second finding, that shows that the crystals spacings are not randomly distributed in the Koi fish system, is the value of the nearest neighbor autocorrelation function, which determines the correlation between the spacings of neighboring crystals. We have found the Koi fish system to have around 60% correlation. In our simulations we found that adding this correlation produces a more uniform reflectance across the whole visible range, in agreement with silvery reflectance. The irregularities in the fish scale system, make it possible to reflect light over a much broader range of angles. This effect might be important for camouflage in aqueous environments in which light scattered in the water hits the scale surface at a wide range of angles. These structures also allow the system to be much more tolerant toward imperfections in the manufacture and assembly process. Nevertheless, the regulated intracellular crystal formation mechanism results in some intrinsic order. The fine balance between order and disorder in this photonic structure produces the observed broad angle silvery iridescence.

The use of materials showing iridescence, especially biocompatible materials, has rapidly increased in the last couple of decades. However, one fundamental industrial requirement to enhance their brilliance is still commonly achieved by mixing the materials with metal-based pigments.[18,35,36] The Gin Rin system may present a different solution to this issue by enhancing silvery reflectance without introducing extra steps and new materials to the system.

CONCLUSIONS

Fish evolved different solutions to enhance the reflectance of their scales. The higher reflectance intensity in the Gin-Rin relative to the Common Koi is mainly achieved by the higher coverage area of the crystal stacks and by increasing the number of reflecting units. In addition, by varying the angle of the crystals relative to the surface and by promoting the interdigitation of the crystal stacks, the thickness of the crystal stacks is reduced, and disorder in the crystal spacings is introduced, thus efficiently enhancing reflectance.

EXPERIMENTAL SECTION

Fish. Koi fish Platinum Ogon and Platinum Ogon Gin Rin were provided by the Gan Shmuel Fish Breeding Center (Kibbutz Gan Shmuel, Israel) or by Peka (Rehovot, Israel) and were maintained in an aquarium.

Reflectance Measurements. The reflectance of scales of around 3 × 4 mm^2 in area and 200 μm in thickness was measured from 2 Common Koi and 2 Gin Rin Koi (3 scales from each fish) within 1 h after extraction of the scale from the fish. We used a custom built microscope for measuring the reflectance, consisting of a micro-spectrophotometer, two CCD cameras, and a high numerical aperture objective (Figure 6). The custom built microscope enabled us to acquire the reflectance spectrum and image of the epidermal layer and its associated scale as well as to obtain the Fourier transform of the reflectance for the same location in the scale. The reflectance spectrum and the image acquired by the microscope were used to determine the reflectance intensity, which was normalized to the reflectance of a silver mirror and to the coverage area of the crystal stacks beneath the scale. The coverage areas were determined from the light microscope images by integrating all of the areas covered with crystal stacks. The Fourier transformation of the images was obtained in order to verify that most of the highly spread reflected light from the scale and skin was indeed collected (Figure 2S). The fish scales and underlying skin used were similar in size and had a silvery iridescence with no observable pigments which might affect their reflectance. The light source used was a Halogen lamp that was coupled to an optical fiber which guided the light into the microscope. The light was then imaged (through a beam splitter) onto the back aperture of an objective (Olympus, UPLSAPO 60XW, NA 1.2). The objective was used both to illuminate a wide area (~250 μm width) and to collect the scattered light. The collected light was directed to one of three different paths by a set of folding mirrors. In the first path, the sample was imaged onto a CCD camera (Mintron, MTV 13 V5Hc).

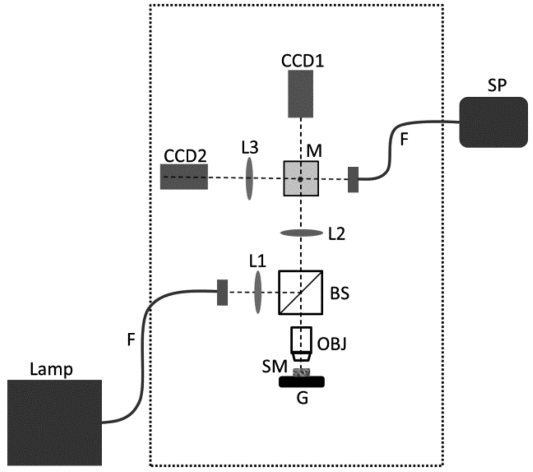

Figure 6. Schematics of the optical setup. The light from a Halogen lamp is coupled to an optical fiber (F) and guided into a custom-made microscope. The light beam is then focused through a lens (L1) and reflected by a beam splitter (BS) onto the back aperture of a high numerical aperture objective (OBJ). The light illuminates a wide area on the sample (SM), which is placed on a translation and goniometer stages (G). After passing through the tube lens (L2) the light continues in one of three paths as determined by a set of folding mirrors (M). It is either imaged onto CCD1, Fourier transformed onto CCD2, or coupled into an optical fiber (F) which guides it into a spectrometer (SP).

In the second path, the Fourier transform of the scattered light was captured by imaging the back aperture of the objective onto a similar CCD camera. In the third path, the light was collected and coupled into a fiber which guided the light into a spectrometer (Ocean Optics, USB2000). We note that the sample was placed on top of translation and goniometer stages so that both its position and orientation could be controlled.

Cryo-SEM. Scale fragments about 2 × 2 mm^2 were cut from the previously measured freshly collected scales. The samples were immediately immersed in 10% dextran (Fluka) or hexadecene (Sigma-Aldrich), sandwiched between two metal discs (3 mm diameter, 0.1 mm cavities), and cryo-immobilized in a high-pressure freezing device (HPM10; Bal-Tec). The frozen samples were mounted on a holder under liquid nitrogen and transferred to a freeze fracture device (BAF 60; Bal-Tec) by using a vacuum cryo-transfer device (VCT 100; Bal-Tec). Samples were observed in an Ultra 55 SEM (Zeiss) by using a secondary electron in-lens detector and a backscattered electron in-lens detector, maintaining the frozen-hydrated state by use of a cryo-stage operating at a temperature of −120 °C. Measurements of crystal thickness and cytoplasm spacings were performed from the cryo-SEM micrographs choosing the crystals that appeared to be edge-on to the fracture surface. In cases in which adjacent crystals were highly angled one to the other the specific crystal pairs were not selected for cytoplasm measurements.

Simulated reflectivity. For the simulations we assumed that incident light enters normal to the scale. For light entering the scale at an angle of ±30°, we estimate a relative error of up to 10% for the simulated reflectivity. We also assumed that the refractive index is independent from the wavelength and that all the interfaces are parallel. The percent reflectivity was then calculated by averaging 500 runs. The total reflectivity was obtained by integrating the reflectivity over all wavelengths.

Every layer is characterized by n_j (refractive index) and d_j (which is the layer thickness randomly picked from the experimental distribution). Thus, for each layer we define the following 2 × 2 matrix:

$$m_j = \begin{pmatrix} \cos\beta_j & -\frac{i}{n_j}\sin\beta_j \\ -n_j\sin\beta_j & \cos\beta_j \end{pmatrix} \quad \text{where} \quad \beta_j = \frac{2\pi}{\lambda} n_j d_j \tag{1}$$

The set of k double layers is characterized by an overall reflectivity 2 × 2 matrix:

$$M_j = \prod_{j=1}^{j=2k} m_j \tag{2}$$

In the case of the Gin Rin, such a matrix is defined for each of the crystal stacks.

In both cases, Common or Gin Rin the reflectivity is extracted from the following expression:

$$R = \left| \frac{(m_{11} + m_{12}) - (m_{21} + m_{22})}{(m_{11} + m_{12}) + (m_{21} + m_{22})} \right|^2 \tag{3}$$

The refractive index of guanine was taken to be n = 1.83 and of the cytoplasm n = 1.33. The calculation was performed using the observed distribution for each sample as well as the calculated nearest-neighbor correlation of 60%.

The simulation did not take into account the absorption of the scales and skins. We determined that the scales and skins absorb mostly in the region of 360−560 nm and have almost no absorbance at longer wavelengths (Figure S3). This can account for some of the differences observed between the measured and the calculated reflectances.

dx.doi.org/10.1021/ja509340c | J. Am. Chem. Soc. 2014, 136, 17236−17242

■ ASSOCIATED CONTENT

Supporting Information

Details of the nearest-neighbor correlation calculation, Fourier transformation of the reflectance, absorbance spectra of the scale and skin, a table with structural information obtained from cryo-SEM of scales and skins from three additional different fish. This material is available free of charge via the Internet at http://pubs.acs.org.

■ AUTHOR INFORMATION

Corresponding Author

lia.addadi@weizmann.ac.il

Notes

The authors declare no competing financial interest.

■ ACKNOWLEDGMENTS

We thank Dr. N. Stettner and the department of Veterinary Resources, Weizmann Institute (Rehovot, Israel), for maintaining the fish, and Gan Shmuel Fish Breeding Center (Kibbutz Gan Shmuel, Israel) for supplying the fish. We thank Rob Forbis for introducing the Gin Rin Koi to us and for his helpful advice. This research was supported by a grant from Israel Science foundation (grant no. 2012\224330*) and by the Crown Center of Photonics and the ICORE: the Israeli Excellence Center "Circle of Light". L.A. is the incumbent of the Dorothy and Patrick Gorman Professorial Chair of Biological Ultrastructure, and S.W. of the Dr. Trude Burchardt Professorial Chair of Structural Biology.

■ REFERENCES

(1) Herring, P. J. *Comp. Biochem. Physiol., Part A: Mol. Integr. Physiol.* **1994**, *109*, 513.
(2) McKenzie, D. R.; Yin, Y. B.; McFall, W. D. *Proc. R. Soc. London A* **1995**, *451*, 579.
(3) Denton, E. J.; Nicol, J. A. C. *J. Mar. Biol. Assoc. U. K.* **1965**, *45*, 683.
(4) Land, M. *Prog. Biophys. Mol. Biol.* **1972**, *24*, 75.
(5) Denton, E. J. *Philos. Trans. R. Soc. London, Ser. B* **1970**, *258*, 285.
(6) Chiou, T. H.; Kleinlogel, S.; Cronin, T.; Caldwell, R.; Loeffler, B.; Siddiqi, A.; Goldizen, A.; Marshall, J. *Curr. Biol.* **2008**, *18*, 429.
(7) Raabe, D.; Sachs, C.; Romano, P. *Acta Mater.* **2005**, *53*, 4281.
(8) Parker, A. R. *J. Opt. A: Pure Appl. Opt.* **2000**, *2*, R15.
(9) Vukusic, P.; Sambles, J. R.; Lawrence, C. R.; Wootton, R. J. *Nature* **2001**, *410*, 36.
(10) Parker, A. R.; McKenzie, D. R.; Large, M. C. J. *J. Exp. Biol.* **1998**, *201*, 1307.
(11) Doucet, S. M.; Meadows, M. G. *J. R. Soc., Interface* **2009**, *6*, S115.
(12) Cronin, T. W.; Chiou, T.-H.; Caldwell, R. L.; Roberts, N.; Marshall, J. *Proc. SPIE* **2009**, *7461*, 74610C.
(13) Land, M. F.; Nilsson, D.-E. *Animal Eyes*; Oxford University Press: Oxford, U.K., 2012.
(14) Hooke, R. *Micrographia: Or Some Physiological Descriptions of Minute Bodies Made by Magnifying Glasses, with Observations and Inquiries Thereupon*; Dover Publications, 1665.
(15) Rayleigh, L. *Proc. R. Soc. London, Ser. A* **1917**, *93*, 565.
(16) Rayleigh, L. *Philos. Mag.* **1887**, *24*, 145.
(17) Rayleigh, L. *Philos. Mag.* **1919**, *37*, 98.
(18) Kinoshita, S.; Yoshioka, S. *ChemPhysChem* **2005**, *6*, 1442.
(19) Huxley, A. F. *J. Exp. Biol.* **1968**, *48*, 227.
(20) Herring, P. J. *Comp. Biochem. Physiol., Part A: Mol. Integr. Physiol.* **1994**, *109*, 513.
(21) Hirata, M.; Nakamura, K.-i.; Kanemaru, T.; Shibata, Y.; Kondo, S. *Dev. Dyn.* **2003**, *227*, 497.
(22) Fox, D. L. *Animal Biochromes and Structural Colours: Physical, Chemical, Distributional & Physiological Features of Coloured Bodies in the Animal World*; University Press: Cambridge, 1953.
(23) Cunningham, J. T. *J. Mar. Biol. Assoc. U. K.* **1893**, *3*, 111.
(24) Gur, D.; Politi, Y.; Sivan, B.; Fratzl, P.; Weiner, S.; Addadi, L. *Angew. Chem., Int. Ed.* **2013**, *52*, 388.
(25) Levy-Lior, A.; Pokroy, B.; Levavi-Sivan, B.; Leiserowitz, L.; Weiner, S.; Addadi, L. *Cryst. Growth Des.* **2008**, *8*, 507.
(26) Levy-Lior, A.; Shimoni, E.; Schwartz, O.; Gavish-Regev, E.; Oron, D.; Oxford, G.; Weiner, S.; Addadi, L. *Adv. Funct. Mater.* **2010**, *20*, 320.
(27) Denton, E. J.; Land, M. F. *Proc. R. Soc. London, Ser. B* **1971**, *178*, 43.
(28) Jordan, T. M.; Partridge, J. C.; Roberts, N. W. *Nat. Photonics* **2012**, *6*, 759.
(29) Mueller, K. P.; Labhart, T. *J. Comp. Physiol., A* **2010**, *196*, 335.
(30) Chae, J.; Nishida, S. *Mar Biol.* **1994**, *119*, 205.
(31) Chae, J.; Nishida, S. *J. Mar. Biol. Assoc. U. K.* **1999**, *79*, 437.
(32) Lythgoe, J. N.; Shand, J. *J. Physiol.* **1982**, *325*, 23.
(33) Lythgoe, J. N.; Shand, J. *J. Exp. Biol.* **1989**, *141*, 313.
(34) Yoshioka, S.; Matsuhana, B.; Tanaka, S.; Inouye, Y.; Oshima, N.; Kinoshita, S. *J. R. Soc. Interface* **2011**, *8*, 56.
(35) Kinoshita, S.; Yoshioka, S.; Miyazaki, J. *Rep. Prog. Phys.* **2008**, *71*, 076401.
(36) Starkey, T.; Vukusic, P. *J. Nanophotonics* **2013**, *2*, 289.